P H Y S I C A L   R E V I E W   L E T T E R S

Extended Skyrmion Phase in Epitaxial FeGe(111) Thin Films

S. X. Huang[*] and C. L. Chien[†]

Department of Physics and Astronomy, The Johns Hopkins University, Baltimore, Maryland 21218, USA
(Received 4 April 2012; published 26 June 2012)

The Skyrmion state in epitaxial B20 FeGe(111) thin films, determined by the topological Hall effect, is greatly extended in the phase diagram to cover all temperatures up to the Curie temperature $T_C \approx 271$ K and over a wide magnetic field range that includes a zero magnetic field. The properties of the Skyrmion phase can be controlled and manipulated by the film thickness, which has a strong effect on the stabilization of Skyrmions.

Topological concepts have provided a fascinating twist to our understanding of ordering in physics. One intriguing example is the Skyrmion spin texture [1,2], which carries a topological charge and a Berry phase in real space. These nontrivial spin textures are closely related to emergent electromagnetic phenomena [3] and exhibit spectacular dynamic properties [4–6]. Recently, noncentrosymmetric cubic B20 chiral magnets of metallic MnSi, $Fe_{1-x}Co_xSi$, FeGe, and insulating Cu_2OSeO_3 (multiferroic) with broken space-inversion symmetry have received a great deal of attention. Exotic Skyrmion spin textures have been observed in reciprocal space by small-angle neutron scattering [2] and in real space by Lorentz transmission electron microscopy (TEM) [7–10]. In these 2D Skyrmion double-twist textures, the spins twist smoothly along both the radial and angular directions. The spins rotate gradually from spin-down at the center to spin-up at the edge of a Skyrmion along the radial direction and rotate smoothly as a vortex along the angular direction. These nanoscale Skyrmions tend to form a lattice with hexagonal symmetry. The Berry phase acquired by the electrons traversing through a Skyrmion may be exploited in new spintronics devices due to its unusual response to electric charge current and spin current (e.g., five orders lower current density to move a Skyrmion than that required for a spin transfer torque switch of regular ferromagnets) [11–13]. In bulk B20 ferromagnets, noncollinear helical spin structures with wavelength λ_H are favored by the Dzyaloshinskii-Moriya (DM) interaction. Under the DM interaction with a chiral energy of $D\mathbf{M} \bullet (\nabla \times \mathbf{M})$, where D is the Dzyaloshinskii constant, Skyrmion-like spin structures (precursor states) are formed by thermal fluctuations but only in a very small region in the phase space at temperatures T close to, but below, the ferromagnetic transition temperature T_C and with the presence of a magnetic field H [1,2,14]. Such a small region in phase space is unattractive and indeed impedes the exploration of Skyrmion physics. However, the regular Skyrmion phase may be greatly expanded in thin specimens, especially in thin films [7]. In Lorentz TEM studies of $Fe_{0.5}Co_{0.5}Si$ [7], FeGe [8], MnSi [9], and Cu_2OSeO_3 [10], using specimens with thickness

$t < 100$ nm that have been ion-milled from bulk crystals, Skyrmions have been found to stabilize in a much wider (T, H) region than those in bulk crystals. Theoretical studies in chiral magnets indicate that uniaxial distortion can greatly stabilize Skyrmions over a much wider region in phase space, extending to near zero temperature and possibly even at a zero magnetic field [15–20].

These encouraging experimental and theoretical suggestions notwithstanding, studies of the rich physics of Skyrmions have thus far been confined mostly to bulk materials. It is imperative to explore thin films of chiral magnets and explore the modification of the Skyrmion phase. Large epitaxial thin films of specific orientations are particularly beneficial in the absence of large single crystals. For the exploration of new spintronic phenomena in Skyrmions, thin films are also much more useful where patterned structures are essential.

Among the known cubic B20 chiral magnets, FeGe has the highest $T_C \approx 278$ K, with λ_H of about 70 nm along the helical propagation vector, whose direction is temperature dependent [21]. Under a magnetic field of about 300 Oe, the helical spin structure changes into the conical phase with the propagation vector along the field direction [21]. At the saturation field $H_D \approx D^2\mathbf{M}/2A \approx 3$ kOe at low temperatures, where A is the exchange stiffness, the conical phase transforms into ferromagnetic alignment [21]. Similar to MnSi and $Fe_{0.5}Co_{0.5}Si$, bulk B20 FeGe also has a very small (T, H) region for the Skyrmion-like (precursor states) phase [22]. Unlike MnSi and $Fe_{0.5}Co_{0.5}Si$, for which large single crystals exist, only mm-size FeGe single crystals are available. The lack of large single crystals impedes studies of FeGe, despite favorable attributes. We report in this Letter the realization of epitaxial FeGe thin films, with which we show that the Skyrmion structures can be stabilized in a dramatically larger (T, H) region, including a zero magnetic field, even in films with $t > \lambda_H$.

Epitaxial FeGe(111) films, 18–300 nm in thickness, have been grown by magnetron sputtering in a high vacuum chamber (base pressure 3.5×10^{-8} torr) on HF etched undoped Si(111) substrates at a substrate temperature of 500 °C. The $\theta/2\theta$ x-ray diffraction pattern (not

shown) indicates only the B20 FeGe(111) phase with less than 0.5% impurity phases. The out-of-plane lattice constant d_{111} is about 0.5% less than that in bulk and indicates tensile strain. An x-ray diffraction ϕ scan reveals the epitaxial relationship of FeGe[1$\underline{1}$0]∥Si[11$\underline{2}$] with a 30° rotation and twinning, as shown in Fig. 1(a) over the area of 3 cm^2.

Magnetic hysteresis loops at 10 K of the 300-nm FeGe film with in-plane ($H_∥$) and out-of-plane ($H_⊥$) magnetic fields reveal in-plane magnetization favored by shape anisotropy, as shown in Fig. 1(b). The saturation field H_S, defined at the knee point in the M-H curve, is about 1.5 and 7 kOe for $H_∥$ and $H_⊥$, respectively. The in-plane saturation field of 1.5 kOe is considerably smaller than the $H_D \approx$ 3 kOe defined above, suggesting more complex ordering, such as the helicoid phase [19] under $H_∥$. In contrast to those of common ferromagnets such as Fe and Co, the $H_∥$ hysteresis loop of FeGe film shows negligible remanence, a small coercivity, and a slanted loop, features that are likely to be related to the complex domain structures of the helicoids [23–25]. The ac susceptibility measurement with an in-plane ac field of 10 Oe at 913 Hz [inset of Fig. 1(b)]

(a)
FeGe
Si
30°
Counts(a.u.)
φ(°)

(b)
300-nm; T=10K
in-plane
out-of-plane
$H_{∥S}$
$H_{⊥S}$
271K
$M(\mu_B/\text{Fe})$
H(kOe)

(c)
18-nm
30-nm
60-nm
90-nm
125-nm
300-nm
$R(T)/R(300K)$
t(nm)
T(K)

FIG. 1 (color online). (a) In-plane φ scan about the (111) peak of the FeGe(111) film and the Si(111) substrate. (b) Hysteresis loop of 300-nm FeGe film at 10 K. Inset: in-plane ac susceptibility of the FeGe(111) film as a function of temperature. (c) Resistivity ratio $R(T)/R(300\,\text{K})$ as a function of temperature for films with various thicknesses indicated. Inset: resistivity at 300 K as a function of thickness.

gives $T_C \approx 271$ K, slightly lower than that of bulk FeGe. The resistance measurements show that all the FeGe films are metallic displaying a systematic dependence on thickness. The high resistance ratio $R(300\,\text{K})/R(10\,\text{K})$ of 7 for the 300-nm film suggests high quality FeGe(111) epitaxial films. As shown in the inset of Fig. 1(c), the resistivity at room temperature of the FeGe thin films varies little for the thick films but increases sharply at small thicknesses as interfacial scattering sets in.

The Skyrmion spin texture in B20 chiral magnets has a Skyrmion number of -1 [2], where each Skyrmion quantizes with an emergent gauge flux of 2 flux quanta ($2\phi_0 = h/e$) [8]. This quantization produces a fictitious magnetic field of $B_{\text{eff}} = 2\phi_0/A$, where A is the area of the Skyrmion that deflects electrons and leads to the topological Hall effect (THE) [26,27]. Numerous experiments [12,28–30] have demonstrated that the THE is strong evidence, indeed a hallmark, for the existence of Skyrmions. The total Hall resistivity ρ_H is then [30]

$$\rho_{yx} = \rho_H = R_0 H + R_S M + \rho_{TH}, \qquad (1)$$

where R_0 is the ordinary Hall coefficient, R_S is the anomalous Hall effect coefficient, ρ_{TH} is the topological Hall resistivity due to the Skyrmion spin texture, and H is perpendicular to the film plane. In Eq. (1), the magnetization value M includes only that of the sample with the substrate contribution separately measured and subtracted. It turns out that the analysis of extracting ρ_{TH} is insensitive to any residue linear M-H contribution, which affects the value of R_0 but not those of ρ_{TH}. While R_S may be a complex function of resistivity ρ (e.g., $a\rho + b\rho^2$) [31], in our case, the magnetoresistance is so small (less than 0.5%) that the detailed mechanisms for the anomalous Hall effect are irrelevant (R_S is nearly a constant with a magnetic field). For simplicity, we adopt $R_S = S_A \rho^2$, as in previous works, where S_A is independent of a magnetic field [30,32]. At large H, ρ_{TH} vanishes when all the spins are aligned. Following previous analyses [30], by a linear fitting of ρ_H/H vs $\rho^2 M/H$ at large fields, we obtained the coefficients R_0 and S_A. The resistivity ρ_{TH} due to the THE can then be obtained by subtracting ($R_0 H + R_S M$) from ρ_H. The value S_A obtained for the FeGe thin films is positive, whereas it is negative for MnSi [32] and positive for Fe$_{1-x}$Co$_x$Si [33]. As shown in Fig. 2(a) (field sweeps from positive to zero), at high fields of $H > H_{Skx} \approx$ 14 kOe, the calculated and experimental ρ_H results agree excellently.

The experimental ρ_H data (black line, bottom curve from the left) for the 60-nm FeGe film measured at 10 K are shown in Fig. 2(a). The calculated $R_0 H + R_S M$ values (red line, middle curve from the left) using the best-fit values of R_0 and R_S also increase monotonically with H and coincide with ρ_H (black line, bottom curve from the left) at high fields after the THE has been eliminated. By subtracting ($R_0 H + R_S M$) (red line, middle curve from the
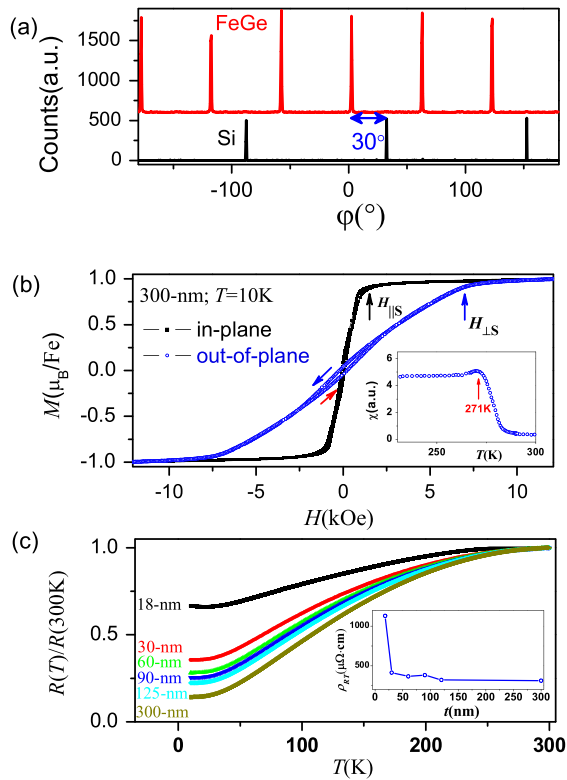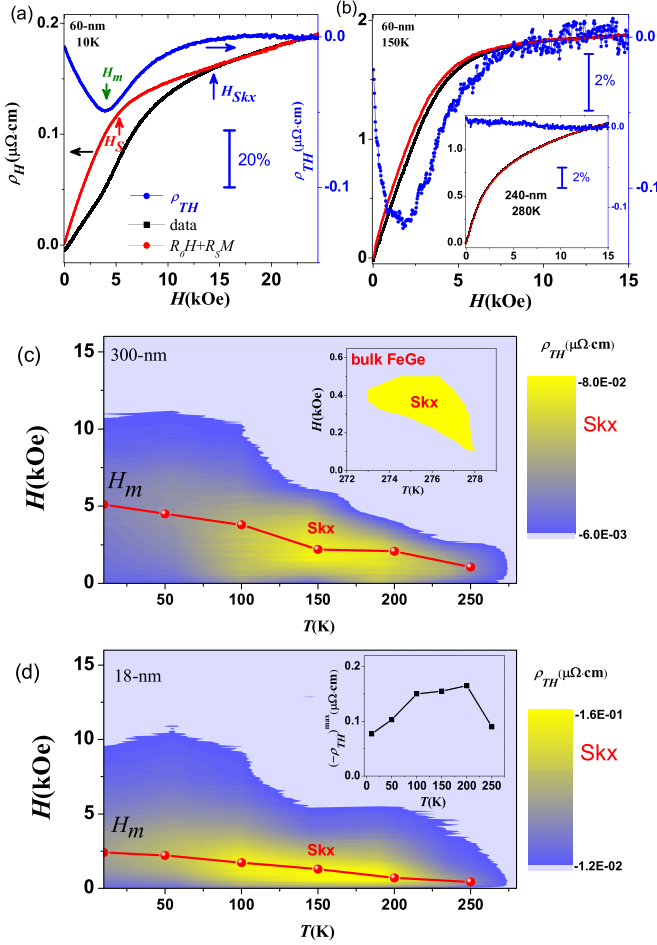
FIG. 2 (color online). Hall resistivity as a function of field for (a) 60-nm film at 10 K and (b) 60-nm film at 150 K. Inset: 240-nm film at 280 K, showing experimental ρ_H (black line, bottom curve from the left) and calculated (red line, middle curve from the left) values of $R_0H + R_SM$, according to Eq. (1), and the topological Hall resistivity ρ_{TH} (blue line, top curve from the left). Color map of topological Hall resistivity in the H-T plane for (c) 300-nm and (d) 18-nm film and the values of H_m. Inset of (c): Skyrmion-like (precursor states) region for bulk FeGe from Ref. [22]. Inset of (d): maximum values of $(-\rho_{TH})$ as a function of temperature.

left) from the experimental ρ_H data (black line, bottom curve from the left), we obtain the THE contribution ρ_{TH} (blue line, top curve from the left), which shows a dome with a minimum at H_m. Such a dome shape of ρ_{TH} centered at H_m is unique to the THE and has been observed in previous experiments [28–30] and described in theories [34]. Lorentz TEM measurements [7,8] with an out-of-plane field reveal the evolution of the magnetic phases culminating with the formation of the Skyrmion lattice at H_m. Below H_m, the stripe domain (helicoid) and Skyrmions coexist, whereas H higher than H_m suppresses the Skyrmion phase and eventually leads to the fully magnetized state. Interestingly, the value of H_{Skx} is much larger than that of H_S. This is likely due to the formation of

free isolated (repulsive) Skyrmions, which are excitations of the saturated state and exist as topologically stable 2D solitons at fields far above H_S, as predicted in theory [19].

To describe the relative magnitude of the THE, we use $THR_m = \rho_{TH}(H_m)/\rho_H(25\ \text{kOe})$, the ratio of $\rho_{TH}(H_m)$ at the peak of the dome and the Hall resistivity $\rho_H(25\ \text{kOe})$ at a large field when the THE is absent. We have found $THR_m \approx 25\%$ at 10 K and decreasing to 6% at 150 K, at which R_0H is less than 1% of ρ_H. For all the FeGe films presented here, ρ_{TH} shows a similar THE dome structure with THR_m larger than 20% at 10 K. At temperatures larger than T_C, e.g., 280 K, there is no THE, as shown in Fig. 2(b). The values of $R_0H + R_SM$ coincide with the experimental data (within 1%) at all magnetic fields.

We determine the Skyrmion phase diagram according to the measured ρ_{TH} for the epitaxial FeGe films. In bulk FeGe, there is a tiny Skyrmion-like (precursor) region in the phase space within the temperature range of $\Delta T \approx$ 273–278 K and the field range of $\Delta H \approx 0.1$–0.5 kOe, as shown in the inset of Fig. 2(c). In contrast, as shown in Figs. 2(c) and 2(d), the Skyrmion region (T, H) in FeGe thin films, illustrated by the 18-nm and 300-nm samples, is dramatically expanded to cover essentially the entire temperature range from low temperatures to T_C. Furthermore, in bulk FeGe, the Skyrmion state emerges only under a magnetic field, since the ground state is the conical (helical) state. In FeGe thin film, the Skyrmion state *exists* in the ground state even at a zero magnetic field. At 10 K, the magnetic field range has extended to more than 10 kOe. Within the Skyrmion phase, ρ_{TH} varies systematically and reaches a maximum in the vicinity of 150 K, at which $\rho_{TH} = 0.16$ and 0.08 $\mu\Omega \cdot$ cm for the 18-nm and 300-nm films, respectively. The THE resistivity, due to the fictitious magnetic field as a result of the Skyrmion spin textures, is $\rho_{TH} = n_{Skx}PR_0B_{\text{eff}}$ [27,28], where n_{Skx} is the relative Skyrmion density (for compact arrays, $n_{Skx} = 1$) and P is the local spin polarization. For FeGe, B_{eff} is about 1 T if we take the Skyrmion size as 70 nm. The value of $R_0 = 0.072\ \mu\Omega \cdot$ cm/T, measured well above T_C at $T = $ 380 K for the 300-nm film, gives a value of $R_0B_{\text{eff}} = $ 0.072 $\mu\Omega \cdot$ cm, in good agreement with the experimental value of 0.08 $\mu\Omega \cdot$ cm. For a thinner film (18-nm), the Skyrmion size may be smaller [35], thus resulting in larger B_{eff} and ρ_{TH}. Assuming that P, R_0, and B_{eff} are independent of temperature, the variation of ρ_{TH} reflects that of n_{Skx}. This variation of n_{Skx} is in good agreement with the Lorentz TEM measurement of a wedged FeGe thin specimen (15- to 75-nm wedge in thickness by ion milling of polycrystalline FeGe) [8], where n_{Skx} reaches a maximum at around 150–200 K in the intermediate fields and is smaller at low temperature for the 15-nm region. However, for the 75-nm ($\sim \lambda_H$) region, Skyrmions exist only in a very small (T, H) region close to T_C [8]. In our epitaxial thin films, even for the 300-nm film ($\sim 4\lambda_H$), Skyrmions exist in a much extended (T, H) region, essentially over

the entire temperature range below T_C. In recent Lorentz TEM studies of MnSi and Cu_2OSeO_3 at which the thicknesses of thin specimens are 2–3 times their wavelengths, the Skyrmion phases also exist in a much extended (T, H) region [9,10].

In Figs. 2(c) and 2(d), the solid lines indicate the values of H_m at various temperatures. It is noted that the H_m value for the 300-nm film is about twice the value for the 18-nm film; i.e., the thicker film has a larger Skyrmion region, in contrast to that in Ref. [8]. To understand the underlying mechanism for stabilizing Skyrmions in thin films, we have carried out measurements of thin films of various thicknesses from 18 to 300 nm. The field dependence of the THR [$= \rho_{TH}/\rho_H(25 \text{ kOe})$] shows a systematic variation with thickness, as shown in Fig. 3(a), where H_m, at the bottom of the dome, progressively shifts to higher H for increasing t, thus confirming a larger Skyrmion region in thicker films.

Theories suggest that the uniaxial anisotropy in B20 chiral magnets plays an essential role [15–19] in the stabilization of Skyrmions. The uniaxial anisotropy K ($K > 0$, favoring perpendicular magnetic anisotropy

with an energy of $-KM_z{}^2$) and "effective stiffness" K_0 of the conical phase can be calculated from the in-plane and out-of-plane saturation fields $H_{\parallel S}$ and $H_{\perp S}$ [20]:

$$K = -\frac{M_S}{3}\left(H_{\perp S} - H_{\parallel S} - 4\pi M_S - \frac{K_m}{M_S}\right),$$

$$K_0 = \frac{M_S}{6}\left(H_{\perp S} + 2H_{\parallel S} - 4\pi M_S + \frac{2K_m}{M_S}\right), \quad (2)$$

$$K_m = M_s^2 \frac{\lambda_H}{t}[1 - \exp(-2\pi t/\lambda_H)].$$

In the case of 300-nm film, we obtain $K/K_0 \approx 0.02$. As shown in the inset of Fig. 3(a), K increases for decreasing thickness t and reaches to 1.1 for $t = 18$ nm. The increasing perpendicular magnetic anisotropy, as in other magnetic thin films, may originate from surface effects and/or magnetoelastic anisotropy [36] and requires further studies.

The stabilization of Skyrmions in our epitaxial films and the dependence of H_m on t are likely due to the positive K as suggested in theoretical calculations [18]. The conical phase is suppressed due to the increasing DM energy under a positive K, whose magnitude can be as low as $0.05K_0$. As a result, Skyrmions have the lowest energy under a positive K and a magnetic field. A larger K (up to $\sim 2.5K_0$) requires a smaller magnetic field (H_m) to "trigger" the Skyrmion lattice and results in a smaller H-T region of the Skyrmion phase [18]. Our experimental results are consistent with the theoretical phase diagram in Ref. [18]. As shown in Fig. 3(b), the largest ρ_{TH} occurs at the smallest t, perhaps due to the smaller Skyrmion size in thinner films [35].

As shown in Figs. 2 and 3, when the magnetic field is swept from positive to zero, the topological Hall resistivity reduces to a small but negative value at a zero magnetic field. The nonzero ρ_{TH} at a zero field observed in our epitaxial films, which is not observed in bulk samples [28–30], may come from the pinning of Skyrmions by grain boundaries, such as the "half-Skyrmion-like" structure pinned at the grain boundary at a zero field observed in Lorentz TEM experiments [8]. This result suggests not only the existence of Skyrmions at a zero field but also the unusual behavior at $H = 0$ between the H-increasing and the H-decreasing branches. In Fig. 1(a), the magnetization of FeGe film shows a normal counterclockwise hysteresis loop with a small positive remnant magnetization M_r when H is swept from large positive H to zero, which is denoted as $H = 0^+$. From Eq. (1), the Hall resistivity at $H = 0^+$ is $\rho_H(0^+) = R_S M_r + \rho_{TH}(0^+)$, which is negative because M_r is small, and $\rho_{TH}(0^+) < 0$ as shown in Fig. 3(a). By the same token, when H is swept from large negative H to zero, denoted as $H = 0^-$, $\rho_H(0^-) = -\rho_H(0^+) > 0$. As a result, the Hall resistivity shows a hysteresis loop that is clockwise, as shown Fig. 4.

In summary, despite existing in a very small region of the phase space in bulk FeGe, the Skyrmion phase has been greatly expanded in epitaxial FeGe(111) thin films, in
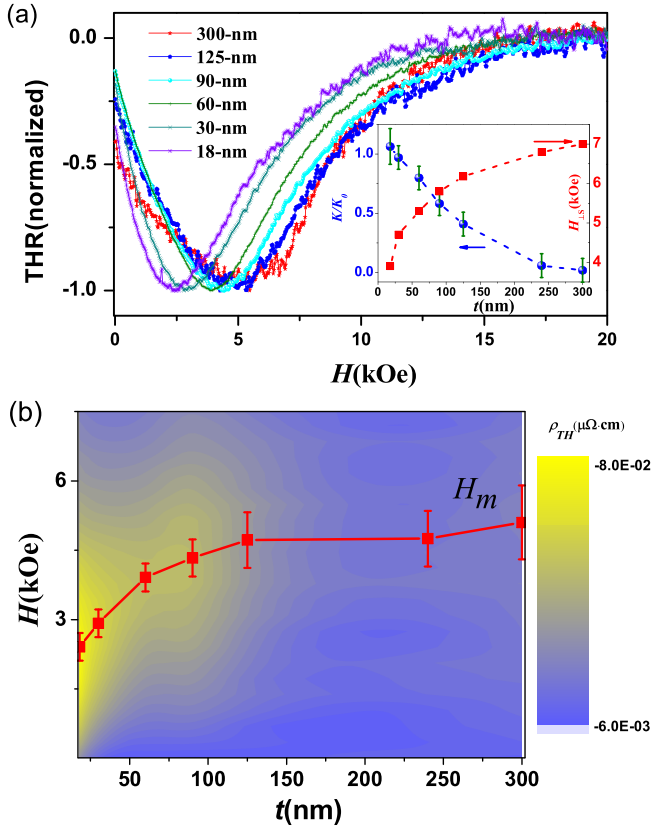

FIG. 3 (color online). (a) Normalized THR = $\rho_{TH}/\rho_H(25 \text{ kOe})$ as a function of a magnetic field for various thicknesses at 10 K. Inset: K/K_0 and $H_{\perp S}$ as a function of thickness t. (b) Color map of topological Hall resistivity in the H-t plane at $T = 10$ K; square symbols are the values of H_m.
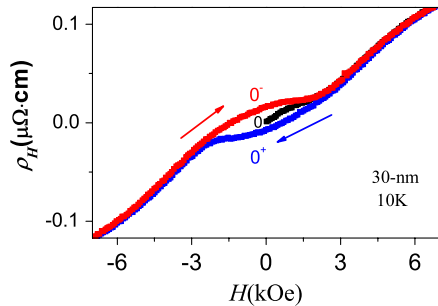
FIG. 4 (color online).   Hall resistivity hysteresis loop for 30-nm films at 10 K.

agreement with theoretical studies [15–19]. In FeGe thin films, the Skyrmion phase exists over the entire temperature range up to T_C and over a wide magnetic field range that includes a zero field. The Skyrmion phase is present in films from 18 nm to at least 300 nm, which is several times the wavelength. Epitaxial Skyrmion thin films open the way for studies of Skyrmions, the manipulation of their properties, and the exploration of new spintronic properties of Skyrmions.

---

*sxhuang@pha.jhu.edu
†clc@pha.jhu.edu

[1] U. K. Roszler, A. N. Bogdanov, and C. Pfleiderer, Nature (London) **442**, 797 (2006).
[2] S. Mühlbauer, B. Binz, F. Jonietz, C. Pfleiderer, A. Rosch, A. Neubauer, R. Georgii, and P. Böni, Science **323**, 915 (2009).
[3] N. Nagaosa and Y. Tokura, Phys. Scr. **T146**, 014020 (2012).
[4] O. Petrova and O. Tchernyshyov, Phys. Rev. B **84**, 214433 (2011).
[5] M. Mochizuki, Phys. Rev. Lett. **108**, 017601 (2012).
[6] Y. Onose, Y. Okamura, S. Seki, S. Ishiwata, and Y. Tokura, arXiv:1204.5009.
[7] X. Z. Yu, Y. Onose, N. Kanazawa, J. H. Park, J. H. Han, Y. Matsui, N. Nagaosa, and Y. Tokura, Nature (London) **465**, 901 (2010).
[8] X. Z. Yu, N. Kanazawa, Y. Onose, K. Kimoto, W. Z. Zhang, S. Ishiwata, Y. Matsui, and Y. Tokura, Nature Mater. **10**, 106 (2011).
[9] A. Tonomura, X. Yu, K. Yanagisawa, T. Matsuda, Y. Onose, N. Kanazawa, H. S. Park, and Y. Tokura, Nano Lett. **12**, 1673 (2012).
[10] S. Seki, X. Z. Yu, S. Ishiwata, and Y. Tokura, Science **336**, 198 (2012).
[11] F. Jonietz et al., Science **330**, 1648 (2010).
[12] T. Schulz, R. Ritz, A. Bauer, M. Halder, M. Wagner, C. Franz, C. Pfleiderer, K. Everschor, M. Garst, and A. Rosch, Nature Phys. **8**, 301 (2012).
[13] J. Zang, M. Mostovoy, J. H. Han, and N. Nagaosa, Phys. Rev. Lett. **107**, 136804 (2011).
[14] C. Pappas, E. Lelièvre-Berna, P. Falus, P. M. Bentley, E. Moskvin, S. Grigoriev, P. Fouquet, and B. Farago, Phys. Rev. Lett. **102**, 197202 (2009).
[15] A. Bogdanov and D. Yablonsky, Sov. Phys. JETP **68**, 101 (1989).
[16] A. Bogdanov and A. Hubert, J. Magn. Magn. Mater. **138**, 255 (1994).
[17] A. Bogdanov and A. Hubert, J. Magn. Magn. Mater. **195**, 182 (1999).
[18] A. B. Butenko, A. A. Leonov, U. K. Rößler, and A. N. Bogdanov, Phys. Rev. B **82**, 052403 (2010).
[19] U. K. Rößler, A. A. Leonov, and A. N. Bogdanov, J. Phys. Conf. Ser. **303**, 012105 (2011).
[20] E. A. Karhu, U. K. Rößler, A. N. Bogdanov, S. Kahwaji, B. J. Kirby, H. Fritzsche, M. D. Robertson, C. F. Majkrzak, and T. L. Monchesky, Phys. Rev. B **85**, 094429 (2012).
[21] B. Lebech, J. Bernhard, and T. Freltoft, J. Phys. Condens. Matter **1**, 6105 (1989).
[22] H. Wilhelm, M. Baenitz, M. Schmidt, U. K. Rößler, A. A. Leonov, and A. N. Bogdanov, Phys. Rev. Lett. **107**, 127203 (2011).
[23] M. Uchida, Y. Onose, Y. Matsui, and Y. Tokura, Science **311**, 359 (2006).
[24] M. Uchida, N. Nagaosa, J. P. He, Y. Kaneko, S. Iguchi, Y. Matsui, and Y. Tokura, Phys. Rev. B **77**, 184402 (2008).
[25] F. Li, T. Nattermann, and V. L. Pokrovsky, Phys. Rev. Lett. **108**, 107203 (2012).
[26] J. Ye, Y. B. Kim, A. J. Millis, B. I. Shraiman, P. Majumdar, and Z. Tešanović, Phys. Rev. Lett. **83**, 3737 (1999).
[27] P. Bruno, V. K. Dugaev, and M. Taillefumier, Phys. Rev. Lett. **93**, 096806 (2004).
[28] A. Neubauer, C. Pfleiderer, B. Binz, A. Rosch, R. Ritz, P. G. Niklowitz, and P. Böni, Phys. Rev. Lett. **102**, 186602 (2009).
[29] M. Lee, W. Kang, Y. Onose, Y. Tokura, and N. P. Ong, Phys. Rev. Lett. **102**, 186601 (2009).
[30] N. Kanazawa, Y. Onose, T. Arima, D. Okuyama, K. Ohoyama, S. Wakimoto, K. Kakurai, S. Ishiwata, and Y. Tokura, Phys. Rev. Lett. **106**, 156603 (2011).
[31] N. Nagaosa, J. Sinova, S. Onoda, A. H. MacDonald, and N. P. Ong, Rev. Mod. Phys. **82**, 1539 (2010).
[32] M. Lee, Y. Onose, Y. Tokura, and N. P. Ong, Phys. Rev. B **75**, 172403 (2007).
[33] Y. Onose, N. Takeshita, C. Terakura, H. Takagi, and Y. Tokura, Phys. Rev. B **72**, 224431 (2005).
[34] S. D. Yi, S. Onoda, N. Nagaosa, and J. H. Han, Phys. Rev. B **80**, 054416 (2009).
[35] N. S. Kiselev, A. N. Bogdanov, R. Schäfer, and U. K. Rößler, J. Phys. D **44**, 392001 (2011).
[36] M. T. Johnson, P. J. H. Bloemen, F. J. A. den Broeder, and J. J. de Vries, Rep. Prog. Phys. **59**, 1409 (1996).